

# Thermal Bremsstrahlung photons probing the nuclear caloric curve

D.G. d'Enterria <sup>a,c</sup>, G. Martínez <sup>a</sup>, L. Aphecetche <sup>a</sup>,  
 H. Delagrange <sup>a</sup>, F. Fernández <sup>c</sup>, H. Löhner <sup>b</sup>, R. Ortega <sup>c</sup>,  
 R. Ostendorf <sup>b</sup>, Y. Schutz <sup>a</sup>, H.W. Wilschut <sup>b</sup>

<sup>a</sup>*SUBATECH, 4 rue A. Kastler, 44307 Nantes, France*

<sup>b</sup>*Kernfysisch Versneller Instituut, 9747 AA Groningen, The Netherlands*

<sup>c</sup>*Grup de Física de les Radiacions, Universitat Autònoma de Barcelona, 08193 Cerdanyola del Vallès, Catalonia*

---

## Abstract

Hard-photon ( $E_\gamma > 30$  MeV) emission from second-chance nucleon-nucleon Bremsstrahlung collisions in intermediate energy heavy-ion reactions is studied employing a realistic thermal model. Photon spectra and yields measured in several nucleus-nucleus reactions are consistent with an emission from hot nuclear systems with temperatures  $T \approx 4 - 7$  MeV. The corresponding caloric curve in the region of excitation energies  $\epsilon^* \approx 3A - 8A$  MeV shows lower values of  $T$  than those expected for a Fermi fluid.

*Key words:* Nucleus-nucleus reactions, Hard photons, Caloric curve

*PACS:* 21.65.+f, 13.75.Cs, 24.10.Pa, 25.70.-z

---

## 1 Introduction

The determination of the thermodynamical properties such as temperature, density, and excitation energy of the hot nuclear systems produced in nucleus-nucleus reactions is one of the main goals of heavy-ion (HI) physics. At moderate excitation energies,  $\epsilon^* \approx 3A - 15A$  MeV, the experimental derivation of these observables as well as their correlation is a prerequisite for a quantitative investigation of the nuclear equation of state  $\epsilon = \epsilon(\rho, T)$  in connection with a possible liquid-gas phase transition [1–4]. To date the most unambiguous evidence for such a phase transition in HI collisions is given by the “caloric curve”

---

*Email address:* enterria@in2p3.fr (D.G. d'Enterria).

[1] which relates the thermal energy of an excited nucleus to its temperature,  $\epsilon^* = \epsilon^*(T)$ . For very low  $\epsilon^*$ , the caloric curve of nuclei is found to follow very closely [5] the  $\sim T^2$  Fermi law given by the well-known Bethe formula for the nuclear density of states [6]. Such a trend is maintained at moderately low nuclear excitation energies ( $\epsilon^* \lesssim 3A$  MeV) [7]. In the region  $\epsilon^* \approx 3A - 8A$  MeV, however, the curve flattens [1] suggesting a phase transition (the width of the “plateau” indicating the latent heat related to the phase change). Although such thermodynamical behaviour has also been observed in other microscopic systems such as metallic [8] and hydrogen [9] clusters, the empirical determination (and the theoretical interpretation) of the nuclear caloric curve has been a much debated issue the last years [1–4,10,11]. As a matter of fact, the three experimental methods employed so far to measure the temperatures attained in a reaction do not yield fully equivalent caloric curves. The existing nuclear “thermometers” are based on: (i) the slopes of the kinetic energy spectra of light particles (n, p,  $\alpha$ ) [12], (ii) the double ratios of neighbour isotopes [13], and (iii) the relative populations of excited states [14]. Having in hand an alternative thermometer based on a clean and weakly interacting probe would be extremely useful when searching for signals of the nuclear liquid-gas phase transition. Electromagnetic probes, viz. photons and dileptons, due to their weak final state interaction with the surrounding medium, have long been recognized as the most direct probes of the space-time evolution of the colliding nucleons [15]. In HI reactions at intermediate bombarding energies, two concurrent processes are known to be responsible for hard-photon emission [16]: (i) first-chance (off-equilibrium) collisions between projectile and target nucleons in the first stages of the reaction, and (ii) subsequent  $NN$  collisions in the produced “nuclear fireball” zone. The experimental existence of a second thermal component emitted from the produced hot nuclear sources and accounting for up to 30% of the total photon yield above  $E_\gamma=30$  MeV, has been unambiguously observed recently [17–20]. In this Letter we propose to exploit such radiation as a novel thermometer of hot nuclear matter using a realistic thermal model which reproduces satisfactorily the observed photon spectral shapes and yields. Using such a thermometer we then construct the caloric curve in the region of the expected liquid-gas phase change.

## 2 Thermal model

Photons produced in HI reactions escape freely the interaction region immediately after their production. Thus, even when emitted from an equilibrated source they do not have a blackbody spectrum at the source temperature. However, the inverse slope parameter of their spectrum  $E_0^t$  and the temperature  $T$  of the nuclear medium are strongly correlated. In this work we employ the thermal model of Neuhauser and Koonin [21] (henceforth NK) to quan-

titatively relate  $E_0^t$  and  $T$ . According to this model, the differential rate of photons emitted in incoherent  $NN\gamma$  processes within a hot nuclear fragment is described by the expression:

$$\frac{d^5 N_\gamma}{d^3 x dt dE_\gamma} = 8 \int \frac{d\mathbf{p}_{1i}}{(2\pi)^3} \frac{d\mathbf{p}_{2i}}{(2\pi)^3} f(\mathbf{p}_{1i}) f(\mathbf{p}_{2i}) \beta_{12i} \frac{d\tilde{\sigma}_\gamma}{dE_\gamma}, \quad (1)$$

where  $\mathbf{p}_{1,2i}$  and  $\beta_{12i}$  are the initial momenta and relative-velocity of the colliding nucleons,  $f(\mathbf{p})$  their (single-particle) momentum distribution, and  $d\tilde{\sigma}_\gamma/dE_\gamma$  the angle-integrated *Pauli-blocked*  $NN$  Bremsstrahlung cross-section. Approximating the emitting region as nuclear matter in thermal equilibrium with local temperature  $T$  and density  $\rho$ , the momentum distribution can be simply parametrized by a hot Fermi-Dirac distribution ( $\hbar = c = k_B = 1$ ):

$$f(\mathbf{p}) = \frac{1}{1 + \exp \left\{ \left[ \sqrt{p^2 + m_N^2} - \mu(\rho) \right] / T \right\}}, \quad (2)$$

normalized to  $4 \int d\mathbf{p} f(\mathbf{p}) / (2\pi)^3 = \rho$ . For low temperatures ( $T \ll \epsilon_F$ ) the chemical potential  $\mu$  of a system of nucleons can be written as a function of the Fermi energy  $\epsilon_F(\rho)$  [where  $\epsilon_F = \sqrt{p_F^2 + m_N^2} - m_N$  and  $p_F(\rho) = (3\pi^2 \rho / 2)^{1/3}$ ] and  $T$  [22]:

$$\mu(\rho) \approx \epsilon_F(\rho) \left\{ 1 - \frac{\pi^2}{12} \left[ \frac{T}{\epsilon_F(\rho)} \right]^2 \right\}. \quad (3)$$

The *in-medium* Bremsstrahlung cross-section  $d\tilde{\sigma}_\gamma/dE_\gamma$  of Eq. (1) is approximately [21]

$$\frac{d\tilde{\sigma}_\gamma}{dE_\gamma} \approx \frac{d\sigma_\gamma}{dE_\gamma} \int [1 - f(\mathbf{p}_{1f})] [1 - f(\mathbf{p}_{2f})] \frac{d\Omega_\gamma}{4\pi} \frac{d\Omega_f}{4\pi}, \quad (4)$$

where  $d\sigma_\gamma/dE_\gamma$  is the elementary  $NN$  Bremsstrahlung cross-section in free space,  $[1 - f]$  the usual Pauli-blocking factors, and  $d\Omega_{\gamma,f}$  the solid angle of the outgoing gamma and nucleons. At the considered energies, the reaction  $pp \rightarrow pp\gamma$  is suppressed by a factor  $\sim 20$  with respect to  $pn \rightarrow pn\gamma$  [23], neutron-neutron Bremsstrahlung is vanishingly small, and thus one needs only to consider the  $pn\gamma$  process. The isospin-averaged cross-section  $d\sigma_\gamma/dE_\gamma$  is then one half of  $d\sigma_{pn\gamma}/dE_\gamma$ . We employ here the parametrization of Schäfer *et al.* for  $d\sigma_{pn\gamma}/dE_\gamma$  derived within a proper relativistic and gauge-invariant meson-exchange effective model for the  $NN$  interaction [23], which reproduces well the available data on  $pn$  Bremsstrahlung [24].

## 2.1 Nuclear temperatures

The emission rates given by Eq. (1) can be thus calculated for a nuclear system at temperature  $T$  and density  $\rho$ . The Bremsstrahlung rates are shown in Fig. 1 for a source at  $T = 4, 6$  MeV and  $\rho/\rho_0 = 0.5, 1.0$  ( $\rho_0 = 0.16 \text{ fm}^{-3}$ ). The resulting hard-photon distributions above 30 MeV can be well approximated by a Boltzmann exponential with slope  $E_0^t$  in agreement with the experimental data (Fig. 2). The integrated yields scale approximately with  $T^{6.7}$  and  $\rho$ . The temperature  $T$  of the emitting source and the photon slope parameter  $E_0^t$ , extracted from an exponential fit of the model spectra above  $E_\gamma = 30$  MeV, are found to be well described by the relation:

$$T(\text{MeV}) = (0.78 \pm 0.02) \cdot E_0^t(\text{MeV}), \quad (5)$$

in the range  $T \approx 3 - 10$  MeV and  $\rho \approx (0.3 - 1.2)\rho_0$ .

Applying Eq. (5) the nuclear temperature attained in a HI reaction can be determined by measuring the slope of its thermal hard-photon spectrum. The temperatures obtained for all the systems studied by the TAPS collaboration where a thermal hard-photon component has been measured [17–20] lie in the range  $T \approx 4 - 7$  MeV (Table 1) in agreement with the typical values found in intermediate-energy nucleus-nucleus collisions [2,3]. The highest  $T$  ( $E_0^t$ ) values for a given incident energy  $\epsilon_{lab}$  correspond to the most symmetric systems, which have the highest energy deposition in the center-of-mass,  $\epsilon_{AA} = A_{red} \epsilon_{lab} / A_{tot}$ , i.e., the largest attainable excitation energies. In comparison with the nuclear thermometers used so far [12–14], the thermal-photon thermometer presents several advantages: (i) minimal preequilibrium contamination due to the large difference, by a factor two to three, between the direct (first-chance) and thermal hard-photon slopes [18]; (ii) absence of final-state distortions like side feeding, rescattering, and reacceleration by the Coulomb field and/or collective motion; (iii) measurement of the  $T$  of the system right after equilibration, just before its break-up [19], when the maximum thermal energy of the equilibrated residue is achieved; and (iv) intrinsic selection of (semi)central dissipative reactions with large number of  $NN$  collisions [19]. The use of thermal photon slopes as a nuclear thermometer is however restricted to intermediate-energy reactions with  $\epsilon_{lab} \approx 30A-90A$  MeV. The lower limit in  $\epsilon_{lab}$  results from the experimental difficulty to resolve accurately the thermal component in a double-exponential fit of the hard-photon spectrum due to: (i) the very small cross-section in the direct high-energy region<sup>1</sup>, and (ii) the increasing role at  $E_\gamma < 20$  MeV of statistical  $\gamma$  from decays of Giant Dipole Resonances and bound states. Above  $\epsilon_{lab} \approx 90A$  MeV, hard-photon

<sup>1</sup> The emission probability of a photon of  $E_\gamma > 30$  MeV per  $pn$  collision is a steeply increasing function of the incident energy  $\epsilon_{lab}$  [18]:  $P_\gamma \sim \exp[-(1/\epsilon_{lab})]$ .

spectra are well described by a single “direct” exponential [29,30] and also the background of photons from the decay of the produced  $\pi^0$ 's becomes important [30].

## 2.2 Photon multiplicities

The absolute thermal photon yield per nuclear reaction,  $M_\gamma \equiv \sigma_\gamma/\sigma_{AA}$ , predicted by the NK model can be obtained integrating Eq. (1) over the relevant space-time history of the equilibrated system produced in a nucleus-nucleus reaction:

$$M_\gamma^{\text{NK}} = \int d^3x \int dt \int_{E_\gamma=30 \text{ MeV}}^{\infty} dE_\gamma \frac{d^5 N_\gamma}{d^3x dt dE_\gamma}(T, \rho). \quad (6)$$

In the most general case  $T = T(x, t)$  and  $\rho = \rho(x, t)$ , and the integration in Eq. (6) requires a consistent modeling of the space-time evolution of the reaction as done, e.g., in hydrodynamical approaches. Since we are just interested in verifying that the thermal model provides also a correct estimation of the measured thermal photon yields, we will significantly simplify the calculation of  $M_\gamma^{\text{NK}}$  making a few plausible assumptions. First, one may neglect any  $T$  and  $\rho$  gradients within the nuclear source and approximate the integral over space by the volume of the participant nucleons in the reaction,  $V = A_{\text{tot}}/\rho$ , where  $A_{\text{tot}} = A_1 + A_2$  is the sum of target and projectile nucleons<sup>2</sup>. Secondly, one can simply replace the integral over time by a constant interval equal to the lifetime of the radiating source,  $\Delta\tau \approx 100 \text{ fm}/c$ , consistent with the usual estimates of the lifetime of equilibrated excited nuclei [3]. With these rough approximations, partial integration of Eq. (1) above  $E_\gamma = 30 \text{ MeV}$  permits to compute  $M_\gamma^{\text{NK}}$  straightforwardly. Since the emission rates given by Eq. (1) scale as  $\sim \rho$  and since  $V \propto \rho^{-1}$ , the thermal  $\gamma$  multiplicities are rather insensitive to the density of the source in this very simple estimation. Most experimental multiplicities (Table 1) are very well reproduced by the integrated NK photon rates and our simplified ansatz of the space-time history of the radiating source<sup>3</sup>. The photon yields of the two systems with

<sup>2</sup> The equilibrated nuclear object produced in (semi)central collisions at these energies is likely to include many more constituents than just the original participants as the excitation is shared with other nucleons. Although it is improbable that *all* nucleons are available to participate in the nuclear Bremsstrahlung process (e.g. 10%-20% of them may just be gone in preequilibrium emission), we take here  $A_{\text{tot}} = A_1 + A_2$  as a reliable measure of the (relative) size of the system in the different reactions.

<sup>3</sup> The reported errors on  $M_\gamma^{\text{NK}}$  in Table 1 include the uncertainties in  $T$  propagated from  $E_0^t$  and are quite large due to the strong power dependence of the photon

largest excitation energies ( $^{86}\text{Kr}+^{58}\text{Ni}$  and  $^{36}\text{Ar}+^{58}\text{Ni}$  at  $60A$  MeV), however, are overpredicted by the model (though still within the combined  $M_\gamma^{\text{NK}}$  and  $M_\gamma^{\text{exp}}$  systematic uncertainties). A much better agreement would be reached in these two cases if the lifetime of the equilibrated sources was reduced by a factor  $\sim 2$  compared to lower energies (i.e. if  $\Delta\tau \sim 50$  fm/c). This result is in quantitative agreement with the observed fast break-up of nuclear systems for increasingly larger values of  $\epsilon^*$  interpreted in terms of a low-density (spinodal) fragmentation [31].

### 3 Caloric curve

Having determined the values of  $T$  from  $E_0^t$  through Eq. (5) for our different reactions, a caloric curve  $\epsilon^*(T)$ , can be constructed correlating  $T$  with the *thermal* excitation energies  $\epsilon^*$  attained in each reaction. To construct such a curve, we use the published values of  $\epsilon^*$  measured in semi-central and central reactions with equivalent systems (Table 1, most right column). In the case of  $^{86}\text{Kr}+^{58}\text{Ni}$  at  $60A$ , in the absence of an experimental measurement of  $\epsilon^*$ , an upper value can be obtained from the total (Coulomb-corrected) center-of-mass energy,  $\epsilon_{AA}$ , subtracted of other energy contributions<sup>4</sup>. Although it is fair to acknowledge that our globally indirect determination of  $\epsilon^*$  is potentially subject to significant systematic uncertainties, such uncertainties are reasonably contained in the already intrinsically large experimental errors of the excitation energy measurements [2] and, furthermore, the qualitative conclusions that we obtain from the analysis of the photon caloric curve would only be modified by much larger shifts along the  $\epsilon^*$  axis. The  $\epsilon^* - T$  correlation for the 7 reactions considered here is shown as solid dots in Fig. 3. Our caloric curve falls somewhat above the ALADIN [1] and EOS [32] results<sup>5</sup> obtained with two different isotopic ratios, but still clearly below the region expected for a pure degenerate Fermi fluid (Fig. 3, dark band). The fact that the thermal photon temperatures seem to be slightly larger than the isotopic ones is not surprising since “chemical” temperatures probe a later lower density (cooler) stage when isotopes are produced, whereas the most significant part of thermal photon emission takes place somewhat earlier. Indeed in this

---

emission rates on  $T$ .

<sup>4</sup>  $\epsilon^* \approx (\epsilon_{AA} + Q) - \epsilon_{\text{coll}} - \epsilon_{\text{preeq}} - \epsilon_{\text{rot}}$ , where: (i) the reaction Q-value and  $\epsilon_{\text{rot}}$  are of the order  $\sim 1A$  MeV and have opposite signs, and (ii) the radial flow energy,  $\epsilon_{\text{coll}}$ , and the pre-equilibrium component,  $\epsilon_{\text{preeq}}$ , represent  $\sim 3A$  MeV for a symmetric system at these energies [1–3].

<sup>5</sup> Note however that both, ALADIN and EOS, collaborations have updated slightly upwards their original curves (shown in Fig. 3) to account for several corrections in  $T$  (sequential feedings) and  $\epsilon^*$  (collective radial flow energy), see e.g. [11] for a compilation of the most recent results.

scenario, the radiation of thermal Bremsstrahlung photons occurs during the path followed by the excited nuclear system between the hot “liquid” phase (one single big nuclear fragment at the end of the pure pre-equilibrium stage) and the mixed phase of gaseous particles and small droplets produced later in the fragmentation process [19]. Our caloric curve disagrees, on the other hand, with the one obtained by the INDRA collaboration using kinetic temperatures [10], which follows closely the  $\epsilon^* \sim T^2$  trend. The kinetic  $T$ 's are systematically higher by about 1-2 MeV most likely due to the fact that the slope parameters of  $p$  and  $\alpha$  kinetic energy spectra are influenced by preequilibrium and mid-rapidity emissions [33], and/or nucleon Fermi motion effects. The departure of the photon caloric curve from the  $\epsilon^* = aT^2$  law (with level density parameters  $a = A/8 - A/13 \text{ MeV}^{-1}$ ) characteristic of the nuclear ground state (liquid phase), and the slow increase of  $T$  with  $\epsilon^*$  in the region of intermediate excitation energies are in qualitative agreement with the expected behaviour of a liquid-gas phase transition occurring in excited atomic nuclei.

## 4 Conclusions

A thermal bremsstrahlung model has been employed to extract the thermodynamical properties of the nuclear systems produced in heavy-ion collisions at intermediate-energies. Such a model predicts exponential hard-photon spectra above  $E_\gamma = 30 \text{ MeV}$  in agreement with the experimental data. The thermal slopes are linearly correlated with the temperature of the emitting system. This defines a new thermometer of hot nuclear matter which, at variance with the usual hadronic-based methods, is free of significant final-state distortions. The hot nuclear residues prepared in different reactions with excitation energies  $\epsilon^* \approx 3A - 8A \text{ MeV}$ , have temperatures in the range  $T \approx 4 - 7 \text{ MeV}$  yielding a slowly increasing caloric curve which lies below the expected behaviour for a pure Fermi liquid.

## 5 Acknowledgements

We thank the members of the TAPS collaboration who participated in the KVI and GANIL experimental campaigns in 1997 and 1998. This work has been in part supported by an IN2P3-CICYT agreement, by the Dutch Foundation FOM, and by the European Union HCM network under Contract No. HRXCT94066. D.G. d'E. has been supported by the European Union TMR Programme (Marie-Curie Fellowship No. HPMF-CT-1999-00311).

## References

- [1] J. Pochodzalla, Prog. Part. Nucl. Phys. 39 (1997) 443; J. Pochodzalla et al., Phys. Rev. Lett. 75, (1995) 1040.
- [2] S. Das Gupta et al., nucl-th/0009033.
- [3] J. Richert and P.Wagner, Phys. Rep. 350 (2001) 1.
- [4] “Multifragmentation”, Proc. Int. Workshop XXVII on Gross Prop. of Nuclei and Nuc. Excitations (Hirschegg, Jan. 1999), ed. H. Feldmeier et al. (GSI, Darmstadt, 1999).
- [5] E. Melby et al., Phys. Rev. Lett. 83 (1999) 3150.
- [6] A. Bohr and B. Mottelson, Nuclear Structure, Vol. 1 (World Scientific, Singapore, 1998).
- [7] R. Wada et al., Phys. Rev. C 39 (1989) 497
- [8] M. Schmidt et al., Phys. Rev. Lett. 87 (2001) 203402.
- [9] F. Gobet et al., Phys. Rev. Lett. 87 (2001) 203401.
- [10] Y.G. Ma et al., Phys. Lett. B 390 (1997) 41.
- [11] J.B. Natowitz et al., Phys. Rev. C 65 (2002) 034618
- [12] D.J. Morrissey et al., Annu. Rev. Nucl. Part. Sci. 44 (1994) 27 and references therein.
- [13] S. Albergo et al., Nuovo Cimento A 89 (1989) 1.
- [14] V. Serfling et al., Phys. Rev. Lett. 80 (1998) 3928.
- [15] W. Cassing et al., Phys. Rep. 188 (1990) 363.
- [16] H. Nifenecker and J.P. Bondorf, Nucl. Phys. A 442 (1985) 478.
- [17] G. Martínez et al., Phys. Lett. B 349 (1995) 23.
- [18] Y. Schutz et al., Nucl. Phys. A 622 (1997) 404.
- [19] D.G. d’Enterria et al., Phys. Rev. Lett. 87 (2001) 22701.
- [20] R. Ortega et al., Proc. 6th TAPS Workshop (Krzyze, Sept 2001), to appear in Acta Phys. Pol., nucl-ex/0202027.
- [21] D. Neuhauser and S. Koonin, Nucl. Phys. A 462 (1987) 163.
- [22] J.A. Lopez and C.A. Dorso, Lecture Notes on Phase Transitions in Nuclear Matter (World Scientific, 2000).
- [23] M. Schäfer et al., Z. Phys. A 339 (1991) 391.



- [24] F. Malek et al., Phys. Lett. B 266 (1991) 255.
- [25] J.F. Lecolley et al., Phys. Lett. B 325 (1994) 317; B.M. Quednau et al., Phys. Lett. B 309 (1993) 10.
- [26] R. Sun et al., Phys. Rev. Lett. 84 (2000) 43. The  $\epsilon^*$  values are scaled to account for a slight difference in  $\epsilon_{\text{lab}}$ .
- [27] J. Normand (INDRA collab.), private communication.
- [28] R. Bougault et al., in [4].
- [29] A. Schubert et al., Phys. Rev. Lett. 72 (1994) 1608.
- [30] G. Martínez et al., Phys. Lett. B 461 (1999) 28.
- [31] L. Beaulieu et al., Phys. Rev. Lett. 84 (2000) 5971.
- [32] J.A. Hauger et al., Phys. Rev. Lett. 77 (1996) 235.
- [33] D. Doré et al., Phys. Lett. B 491 (2000) 15.

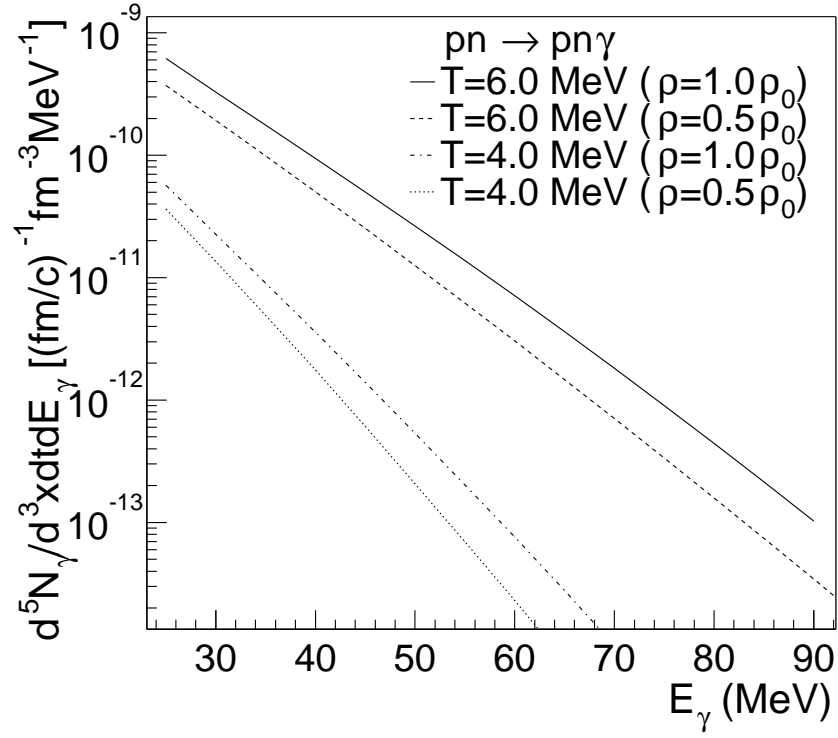


Fig. 1. Thermal Bremsstrahlung emission rates, Eq. (1), given by the NK model for a nuclear system in equilibrium at temperatures  $T = 4, 6$  MeV and densities  $\rho/\rho_0=0.5, 1.0$ .

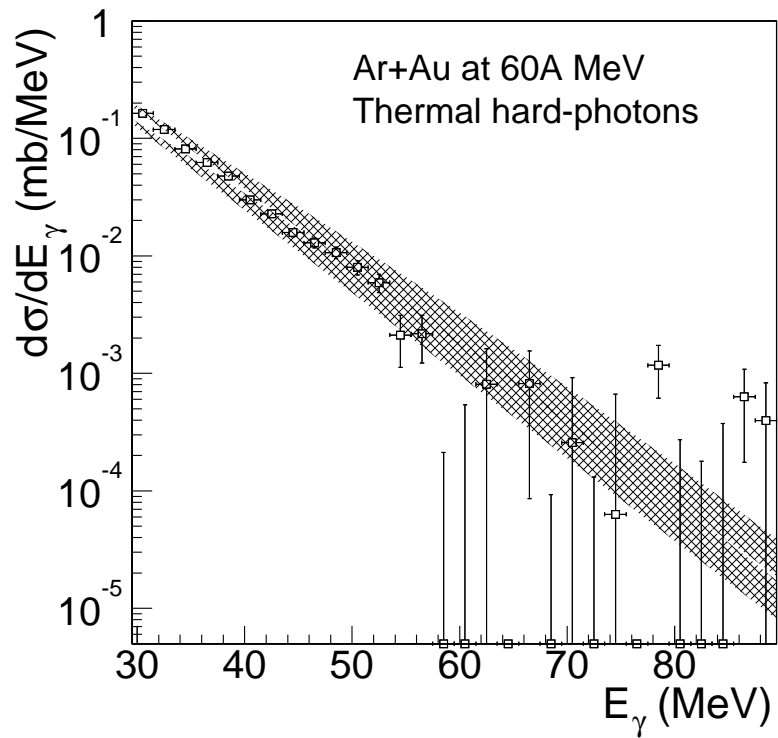


Fig. 2. Thermal hard-photon spectrum measured in the reaction  $^{36}\text{Ar}+^{197}\text{Au}$  at 60A MeV [19] compared (dashed band) to the prediction of the NK model for a source at  $\rho = \rho_0$  and  $T=5.3 \pm 0.5$  MeV (see text and Table 1).

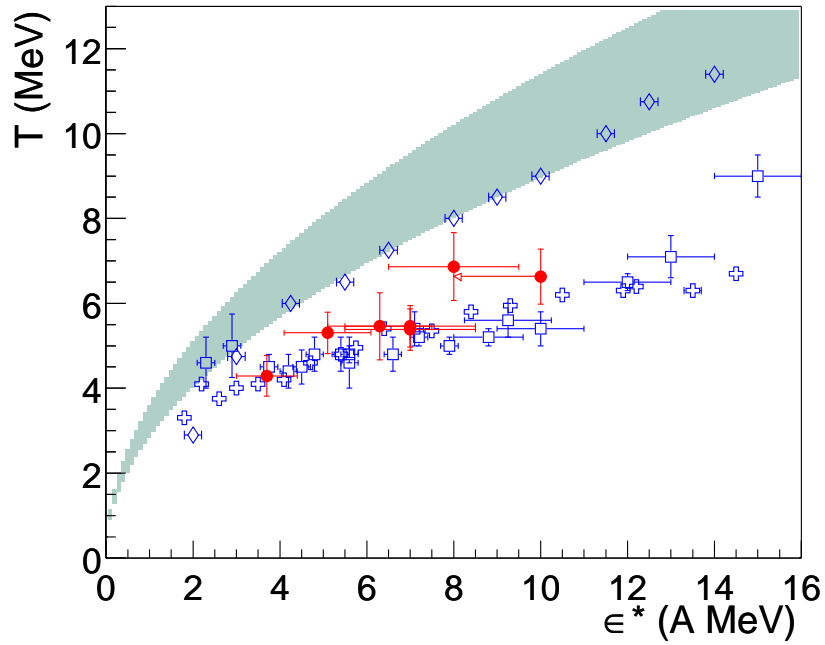


Fig. 3. Caloric curve constructed with the photon slope thermometer (dots) compared to ALADIN (squares) and EOS (crosses) curves (isotopic  $T$ 's), and to INDRA (rhombi) curve (kinetic  $T$ 's). The dark area corresponds to the Fermi relation  $\epsilon^* = aT^2$  with  $a = A/8 - A/13 \text{ MeV}^{-1}$ .

Table 1

Heavy-ion reactions studied by the TAPS collaboration where a thermal bremsstrahlung component has been identified. For each reaction we report: (i) the nuclear temperatures  $T$  extracted through Eq. (5) from the measured thermal slopes  $E_0^t$ ; (ii) the total number of nucleons  $A_{tot}$ , the photon multiplicity  $M_\gamma^{\text{NK}}$  predicted by the NK model (for a source with volume  $V = A_{tot}/\rho$ , and lifetime  $\Delta\tau=100$  fm/c) compared to the experimental value  $M_\gamma^{\text{exp}}$ ; and (iii) the excitation energies  $\epsilon^*$  measured in other experiments.

System	$\epsilon_{\text{lab}}$ (AMeV)	$E_0^t$ (MeV)	$T$ (MeV)	$A_{\text{tot}}$	$M_\gamma^{\text{NK}}$ ( $10^{-4}$ )	$M_\gamma^{\text{exp}}$ ( $10^{-4}$ )	$\epsilon^*$ (AMeV)
$^{208}\text{Pb}+^{197}\text{Au}$	30	$5.5 \pm 0.6$ [17]	$4.3 \pm 0.5$	405	$0.7 \pm 0.7$	$0.6 \pm 0.2$ [17]	$3.7 \pm 0.7$ [25]
$^{36}\text{Ar}+^{197}\text{Au}$	60	$6.8 \pm 0.6$ [19]	$5.3 \pm 0.5$	233	$1.9 \pm 1.3$	$1.6 \pm 0.2$ [19]	$5.1 \pm 1.0$ [26]
$^{181}\text{Ta}+^{197}\text{Au}$	40	$6.9 \pm 0.6$ [17]	$5.4 \pm 0.5$	378	$3.4 \pm 1.9$	$3.2 \pm 1.0$ [17]	$7.0 \pm 1.5$ [27]
$^{36}\text{Ar}+^{107}\text{Ag}$	60	$7.0 \pm 1.0$ [19]	$5.5 \pm 0.8$	143	$1.5 \pm 1.5$	$1.2 \pm 0.2$ [19]	$6.3 \pm 1.2$ [26]
$^{129}\text{Xe}+^{112}\text{Sn}$	50	$7.0 \pm 0.6$ [20]	$5.5 \pm 0.6$	241	$3.1 \pm 2.2$	$2.6 \pm 0.4$ [20]	$7.0 \pm 1.5$ [28]
$^{86}\text{Kr}+^{58}\text{Ni}$	60	$8.5 \pm 0.8$ [17]	$6.6 \pm 0.6$	144	$4.4 \pm 2.7$	$2.0 \pm 0.4$ [17]	<10. (see text)
$^{36}\text{Ar}+^{58}\text{Ni}$	60	$8.8 \pm 1.0$ [19]	$6.9 \pm 0.8$	94	$4.1 \pm 2.9$	$1.1 \pm 0.2$ [19]	$8.0 \pm 1.5$ [26]